

A new studded precast concrete sandwich wall with embedded glass-fiber-reinforced polymer channel sections: Part 1, experimental study

Debrup Dutta, Akram Jawdhari, and Amir Fam

- This paper presents laboratory testing performed on five half-size precast concrete sandwich wall panels to review performance of a new fiber-reinforced-polymer shear connector.
- Research focuses on maximizing degree of composite action, flexural resistance, and thermal efficiency of the connector.
- The studied connector is a commercially available glass-fiber-reinforced polymer channel. For the test panels, the channel flanges were embedded in the concrete wythes in both continuous and discontinuous channel configurations with varying reinforcement ratios.

The use of precast concrete sandwich panels in residential and commercial structures, such as multistory units and warehouses, has grown steadily the past few decades due to their desirable attributes, such as good structural performance, excellent thermal insulation, quality control, speed of construction, versatility, and appealing finishes.¹⁻⁴ Precast concrete sandwich panels typically consist of two reinforced or prestressed concrete layers (also known as wythes) with a thickness of 25 to 100 mm (0.98 to 3.94 in.) and a rigid layer of insulation in between that creates thermal efficiency.⁵

A connector is used to tie the two concrete wythes together and to provide resistance to tensile forces due to stripping, lifting, wind suction, and seismic loads.⁴ In addition, if the wythes are designed to act as partially or fully composite, the connector must be able to transfer some or all of the in-plane shear.³⁻⁵ Conventional connectors consist of discrete ties, bent bars, trusses, grids, expanded perforated plates, or solid concrete zones.^{2,4-6} A high degree of composite action can be achieved by using heavy steel connectors or solid concrete ribs;^{7,8} however, this significantly reduces thermal efficiency because those types of connectors create thermal bridges.⁹ A penetration as small as 2% of the total surface area by steel or concrete connectors can result in a 40% reduction in thermal efficiency.¹⁰

Increasing energy costs, the depletion of resources, and recent calls for sustainable designs make it necessary to seek new types of connectors, such as those made of glass-fiber-reinforced polymer (GFRP) composites. In addition to

PCI Journal (ISSN 0887-9672) V. 65, No. 3, May–June 2020.

PCI Journal is published bimonthly by the Precast/Prestressed Concrete Institute, 8770 W. Bryn Mawr Ave., Suite 1150, Chicago, IL 60631.

Copyright © 2020, Precast/Prestressed Concrete Institute. The Precast/Prestressed Concrete Institute is not responsible for statements made by authors of papers in *PCI Journal*. Original manuscripts and discussion on published papers are accepted on review in accordance with the Precast/Prestressed Concrete Institute's peer-review process. No payment is offered.

their light weight, high tensile strength, and corrosion-resistance characteristics, they are 60 times lower in thermal conductivity than steel connectors.¹¹⁻¹³ Recent research has evaluated the effectiveness of fiber-reinforced polymer (FRP) composites as shear connectors and wythe flexural reinforcement for precast concrete sandwich panels. For example, Salmon et al.⁸ examined various configurations for GFRP connectors, including C- and V-shaped single connectors, and recommended using a continuous truss capable of delivering high composite action. Frankl et al.⁹ conducted four-point bending tests on six full-scale precast, prestressed concrete sandwich panels connected by carbon-fiber-reinforced polymer (CFRP) shear grids. Variables studied in the tests were type of insulation (expanded or extruded polystyrene), wythe and insulation layer thickness, quantity of shear grids, and the contribution of concrete solid regions. The results showed that increasing the relative wythe thickness or quantity of shear grids leads to an increase in the panel stiffness.

Woltman et al.¹³ tested 50 precast concrete sandwich panel segments with dimensions of 254 × 254 × 900 mm (10 × 10 × 35.43 in.) under double-lap shear load. GFRP connectors with different diameters, shapes (circular or rectangular), spacing, and end conditions were used in the tests and were compared with steel and polymer connectors. It was found that the shear strength of GFRP connectors was on average 2.82 times that of commercially available concrete sandwich panel polymer ties but less than that of steel bars. Failure of the GFRP connectors was not governed by pull-out from concrete but by material delamination and longitudinal shear along the connector. The connector shape, diameter, and spacing were found to have negligible effects on the shear strength of the connector. Similarly, GFRP bars were used as shear ties in a flexural study comprising nine full-scale precast concrete sandwich panels under four-point bending.¹⁴ Variables studied were connector diameter and spacing, as well as the contribution of the insulation layer to shear transfer. Increasing the reinforcement ratio of GFRP connectors from 0.026% to 0.098% resulted in increasing load capacity from 58% to 80% of the capacity of an equivalent fully composite panel.¹⁴

Tomlinson et al.³ carried out 38 push-off tests on precast concrete sandwich panel segments connected using basalt-fiber-reinforced polymer (BFRP) bars arranged like a truss. Variables explored were inclination angle of the diagonal members, diameter of the connector, orientation of the connector in relation to the loading direction, and the effects of adhesion and friction bond between the concrete wythes and the insulation layer. Tomlinson and Fam¹⁵ tested five full-scale precast concrete sandwich panels under combined axial and lateral loads. BFRP bars were used as flexural reinforcement for the concrete wythes and as shear connectors. Compared with panels with all-steel reinforcement and connectors, the panels with BFRF bars were 60% to 89% in flexural strength. Similarly, the panels in Tomlinson and Fam,⁵ which were tested under flexural loads only, achieved 75% composite action when BFRP bars were used as con-

nectors only and 55% composite action when they were used as both connectors and wythe reinforcement.

In this paper, a new FRP shear connector is introduced that has similar thermal efficiency to previous FRP connectors while maximizing the degree of composite action and also contributing directly to the flexural resistance. The connector is a commercially available lightweight C-shaped pultruded GFRP channel. By having its flanges embedded in the concrete wythes, the interfacial bond area and, hence, the degree of composite action are expected to increase. Flexural tests were carried out on half-scale panels to evaluate the flexural behavior of precast concrete sandwich panels with the proposed connector, and the bond strength of the concrete-channel interface was evaluated by push-off tests. In the companion paper “A New Studded Precast Concrete Sandwich Wall with Embedded Glass-Fiber-Reinforced Polymer Channel Sections: Part 2, Finite Element and Parametric Studies,”¹⁶ robust nonlinear finite element analyses (FEAs) are presented and used in a comprehensive parametric study that expands the outcome of this study towards meaningful practical recommendations pertaining to the most influential parameters in the proposed system.

Flexural testing program

Panel design and test matrix

Five half-scale panels with dimensions of 3050 × 610 × 280 mm (120.08 × 24.02 × 11.02 in.) (Fig. 1) were cast and tested in four-point bending to evaluate the panel structural performance and degree of composite action achieved using a GFRP channel connector. The thickness of outer and inner concrete wythes was 76 mm (2.99 in.), while the insulation layer of extruded polystyrene (XPS) foam was 127 mm (5 in.) thick (Fig. 1). The insulation block was wrapped with a thin moisture-barrier plastic sheet to act as a bond breaker between concrete and insulation. The goal was to ensure that shear would only be transferred through the channel connector. Adhesion between insulation and concrete, though significant in short-term loading, might not be completely reliable under long-term cyclic and thermal loads.^{3,5,13-15}

The GFRP connector was a 203 mm (7.99 in.) deep C-shaped pultruded channel (Fig. 1), located at midwidth of the specimen and running throughout the length. The channel was centered within the panel thickness so that its flanges were embedded at midthickness of each concrete wythe (Fig. 1). The top and bottom wythe reinforcements lay directly above and below the flanges, respectively, and consisted of welded-steel-wire meshes with a diameter of 5.73 mm (0.23 in.) and spacing of 152 mm (5.98 in.) in both directions.

Test matrix

The test matrix for the flexural tests consisted of five specimens that varied in shear connector and wythe reinforcement ratio (Table 1). The first specimen, CR, had a wythe rein-

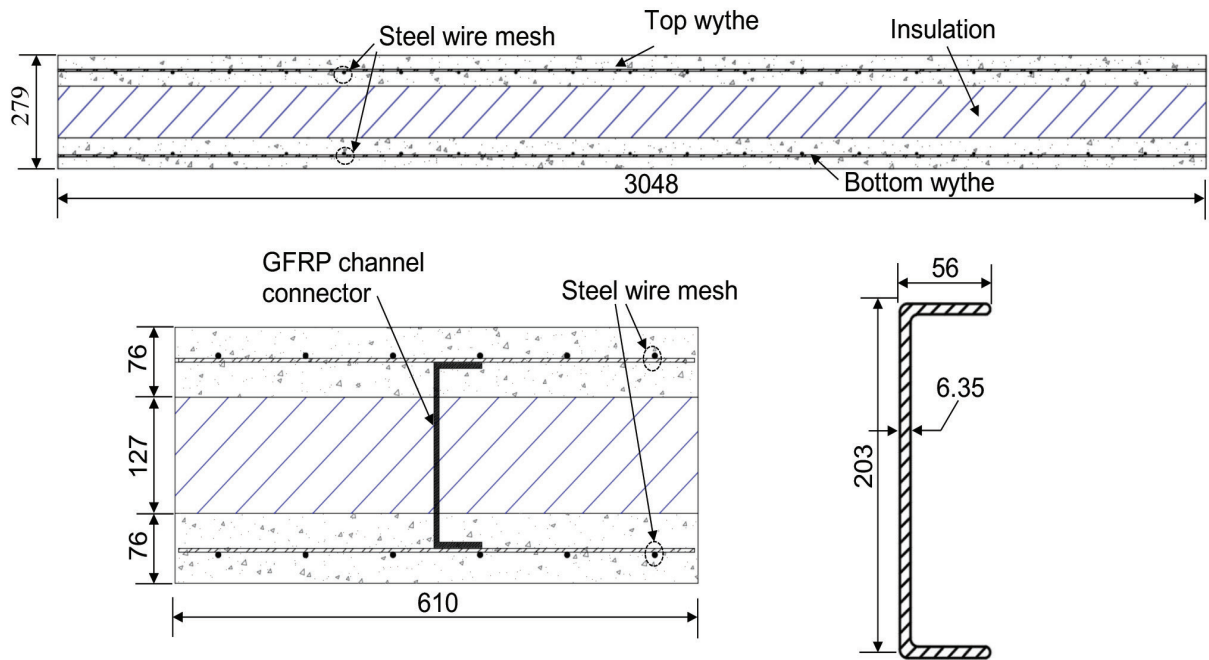


Figure 1. Geometry of test panels shown for elevation (top), panel cross section (bottom left), and glass-fiber-reinforced polymer (GFRP) channel cross section (bottom right). Note: All dimensions are in millimeters. 1 mm = 0.0394 in.

Table 1. Test matrix of flexural concrete sandwich panels

Specimen code	Overall panel dimensions, mm			Wythe reinforcement ratio ρ_s , %	Type of shear connector
	Length	Width	Thickness		
HR	3048	610	279	0.17	Continuous GFRP channel
CR	3048	610	279	0.34	Continuous GFRP channel
DR	3048	610	279	0.68	Continuous GFRP channel
DC	3048	610	279	0.34	Discrete GFRP channel
TR	3048	610	279	0.34	Steel truss

Note: $\rho_s = \frac{A_s}{b \times t} \times 100$, where A_s = area of flexural reinforcement, b = width of concrete wythe, t = wythe thickness. CR = specimen with continuous GFRP shear connectors and a wythe reinforcement ratio equal to 0.34%; DC = specimen with discontinuous GFRP shear connectors and a wythe reinforcement ratio equal to 0.34%; DR = specimen with continuous GFRP shear connectors and a wythe reinforcement ratio equal to 0.68%; GFRP = glass-fiber-reinforced polymer; HR = specimen with continuous GFRP shear connectors and a wythe reinforcement ratio equal to 0.17%; TR = control specimen with steel shear connectors. 1 mm = 0.0394 in.

forcement ratio ρ_s equal to 0.34% of the wythe cross-sectional area, which was identical in both wythes and in the longitudinal and transverse directions. This reinforcement ratio was achieved by using one steel-wire mesh in each wythe. The shear connector in CR was one continuous GFRP channel.

The second and third specimens, HR and DR, were identical to specimen CR, except that the ρ_s was either halved to 0.17% or doubled to 0.68% in specimens HR and DR, respectively, to evaluate the effects of ρ_s . In all specimens, the minimum ρ_s of 0.1% specified by design codes was satisfied.^{4,17} When

reducing ρ_s to one half, the same wire mesh with a diameter of 5.73 mm (0.23 in.) was used, but every other wire in the mesh was removed in both directions. When doubling ρ_s , a second mesh was added in each wythe.

The fourth specimen, DC, had a ρ_s of 0.34% similar to specimen CR, but instead of using a continuous channel connector, multiple discrete (discontinuous) 127 mm (5 in.) long channel segments spaced center to center at 254 mm (10 in.) were used (Fig. 2). The goal was to reduce the web area and, hence, thermal bridging by 50% relative to the full channel and examine its impact on the structural behavior and degree of composite action.

The fifth specimen, TR, which had a conventional steel truss connector (Fig. 2), was used as a control specimen to compare with the four specimens, including the proposed GFRP channel connectors. The steel truss was made by bending a smooth 8 mm (0.31 in.) steel bar 45 degrees diagonally. The 8 mm diameter connector was chosen according to a design criterion of maintaining diagonal stiffness equivalent to the GFRP channel. In the diagonal direction,

the stiffness of the steel bar (area A_s multiplied by elastic modulus E_s) was made equal to the diagonal stiffness of the GFRP channel ($A_{FRP} \times E_{FRP}$), where A_{FRP} is the cross section of the tributary area of the GFRP channel at an angle of 45 degrees (Fig. 3). The band width of the tributary area is defined by the midlength points of two consecutive diagonals normal to the diagonal lying at the center of the band width (Fig. 3).

Materials

Concrete Normal-strength concrete with a design compressive strength f'_c of 30 MPa (4.35 ksi) was used for all panels. Eighteen concrete cylinders measuring 150 × 300 mm (5.9 × 11.8 in.) were prepared and cured according to ASTM C31/C31M¹⁸ and tested according to ASTM C39/C39M.¹⁹ The average 28-day f'_c was found to be 29.2 MPa (4.2 ksi) with a standard deviation of 1.82 MPa (0.26 ksi) and a coefficient of variation of 6.23%. The maximum aggregate size used in the concrete was 14 mm (0.55 in.). A high-range water-reducing admixture was used to increase concrete workability.

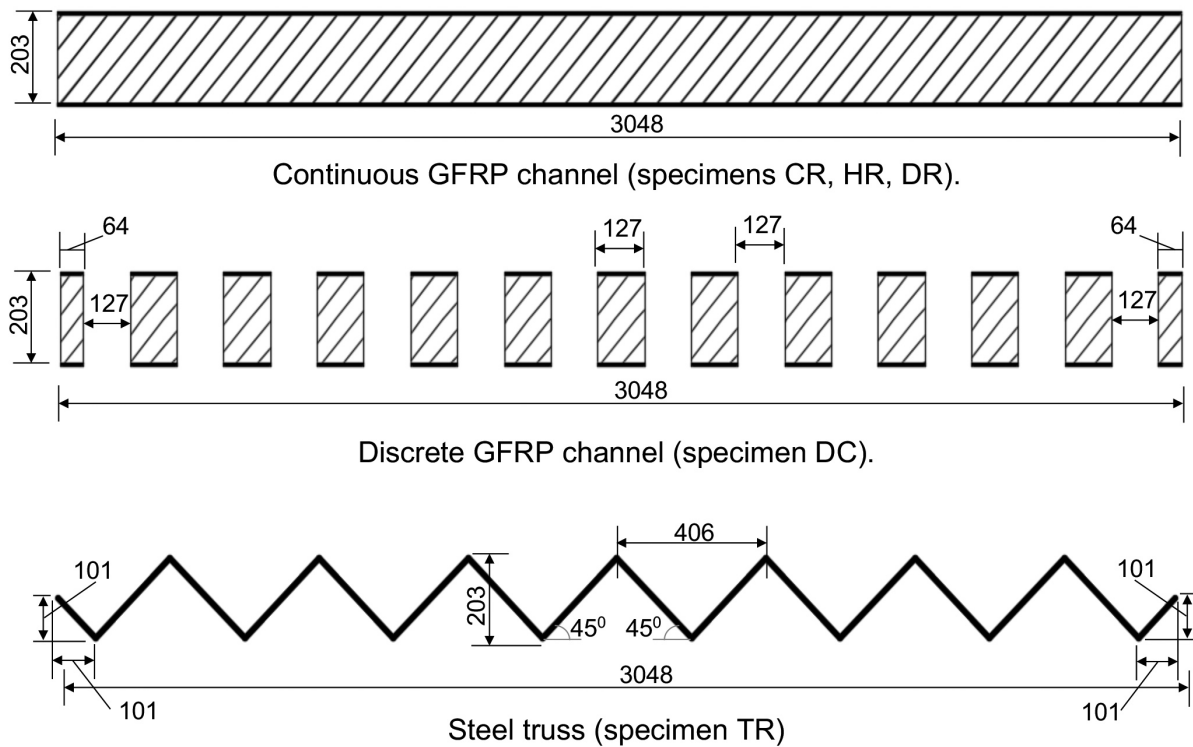


Figure 2. Geometry of various shear connectors used in the bending tests. Note: CR = specimen with continuous GFRP shear connectors and a wythe reinforcement ratio equal to 0.34%; DC = specimen with discontinuous GFRP shear connectors and a wythe reinforcement ratio equal to 0.34%; DR = specimen with continuous GFRP shear connectors and a wythe reinforcement ratio equal to 0.68%; GFRP = glass-fiber-reinforced polymer; HR = specimen with continuous GFRP shear connectors and a wythe reinforcement ratio equal to 0.17%; TR = control specimen with steel shear connectors. All dimensions are in millimeters. 1 mm = 0.0394 in.

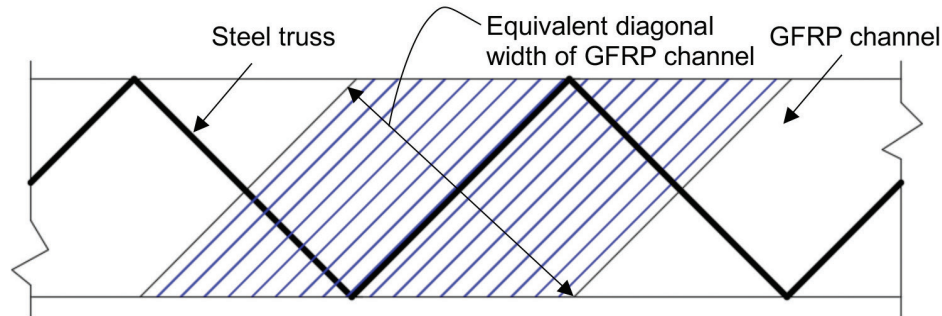


Figure 3. Equivalent diagonal stiffness concept for calculating diameter of steel connector. Note: GFRP = glass-fiber-reinforced polymer.

GFRP channel connector Coupon tests were performed to quantify the tensile strength of the GFRP channel connector in both the longitudinal and transverse directions following ASTM D 3039M.²⁰ The average tensile strength in the fiber direction (longitudinal) was found to be 446 MPa (64.7 ksi) for six coupons taken from the flange and 367 MPa (53.2 ksi) for six coupons taken from the web section. These values are significantly higher than the tensile strength of 207 MPa (30 ksi) reported by the manufacturer. In the transverse direction of the web, the

tensile strength was found to be 123 MPa (17.8 ksi), also higher than the manufacturer-reported value of 48 MPa (6.9 ksi).

The elastic modulus found using strains in the range of 1000 to 3000 $\mu\epsilon$ according to the standard was 26.7 GPa (3872.4 ksi) for the flange in the longitudinal direction, 23 GPa (3336 ksi) for the web in the longitudinal direction, and 9.32 GPa (1351.7 ksi) for the transverse direction of the web. **Figure 4** shows the stress-strain curves, representing the

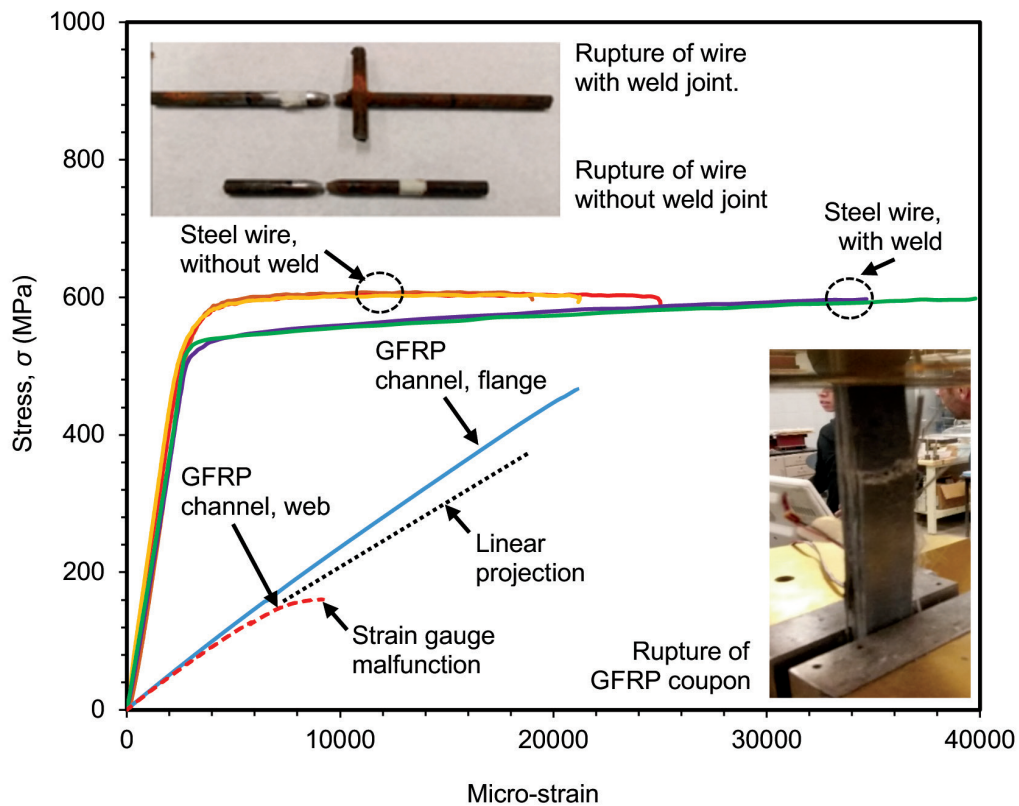


Figure 4. Tensile stress-strain curves for steel reinforcement and GFRP channel connector in the longitudinal direction. Note: GFRP = glass-fiber-reinforced polymer. 1 MPa = 0.145 ksi.

flange and web coupons tested in the longitudinal direction. The channel compressive strength in the longitudinal direction was also quantified experimentally by testing three 51 mm

(2 in.) long full-channel segments. A 6.35 mm (0.25 in.) thick steel plate was used to distribute the load, which was applied to the center of gravity of the cross section to minimize

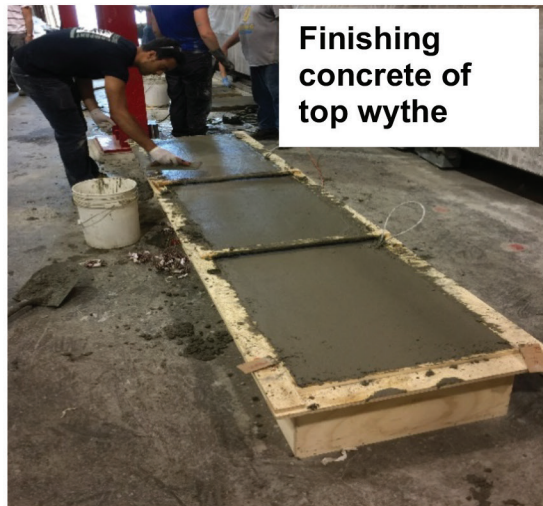
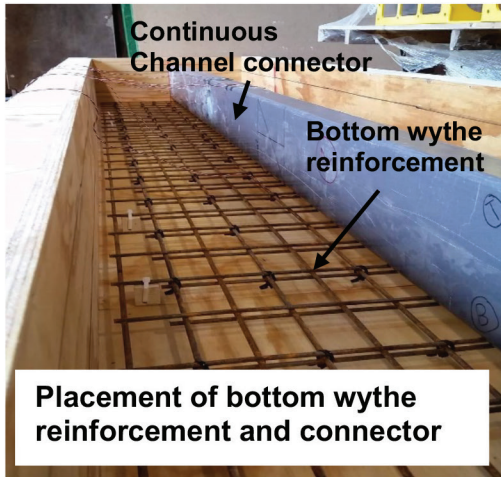


Figure 5. Fabrication of sandwich panels. Note: DC = specimen with discontinuous GFRP shear connectors and a wythe reinforcement ratio equal to 0.34%.

eccentricity. The average compressive strength for the three segments was found to be 186 MPa (27 ksi), slightly less than the 207 MPa (30 ksi) reported by the manufacturer.

Steel In both the steel truss connector and flexural wythe reinforcement, mild steel with a nominal yield strength of 414 MPa (60 ksi) was used. Tensile tests following ASTM A1064/A1064M-18a²¹ were conducted on the steel-wire mesh used as wythe reinforcement. Figure 4 plots the stress-strain curves for the mesh, considering two wire sections, one containing the weld joint and the other without the weld. On average, the yield and ultimate strengths were determined to be 483 and 597 MPa (70 and 86.6 ksi), respectively.

Insulation layer The insulation used in the tests was XPS rigid foam. Earlier tests performed on a similar foam revealed that the foam had compressive and tensile strengths of 0.17 and 0.3 MPa (0.02 and 0.04 ksi), respectively.^{5,13} The density of foam material was 30 kg/m³ (50.625 lb/yd³). According to the manufacturer’s data sheet, the *R*-value, which is a measure of thermal resistance to conductive heat flow, varies from 5.6 to 6.3 m² °C/W (0.99 to 1.11 ft²-h-°F/BTU) depending on the external temperature.

Fabrication

The specimens were fabricated horizontally on level ground using wooden formwork (Fig. 5). The reinforcement of the

bottom wythe was positioned first using plastic chairs to maintain the design concrete cover (Fig. 5). Following positioning and securing of the shear connector on top of the bottom reinforcement, concrete was then placed in the formwork, vibrated, and leveled to a depth of 76 mm (2.99 in.) using a wooden template (Fig. 5).

The insulation blocks, measuring 302 mm (11.89 in.) wide by 127 mm (5 in.) deep by 3048 mm (120 in.) long, were wrapped with moisture-barrier sheets and placed on either side of the channel. Then, the space between the insulation blocks and formwork was sealed before casting the top wythe. The reinforcement mesh for the top wythe was then positioned so that it was resting on plastic chairs and concrete was placed, vibrated, and leveled to a depth of 76 mm (2.99 in.) (Fig. 5). The specimens were covered with wet burlap and sprayed continuously with water for a period of three days after fabrication for concrete curing.

Loading setup and instrumentation

The panels were tested in a four-point bending configuration with a constant moment zone of 500 mm (19.7 in.) and a total span of 2890 mm (113.8 in.) (Fig. 6). The load was applied through stroke control at a rate of 2 mm/min (0.08 in./min) using a 900 kN (202.3 kip) capacity testing machine. Several linear potentiometers were used to measure the deflection at midspan, the slip between the top and bottom wythes at

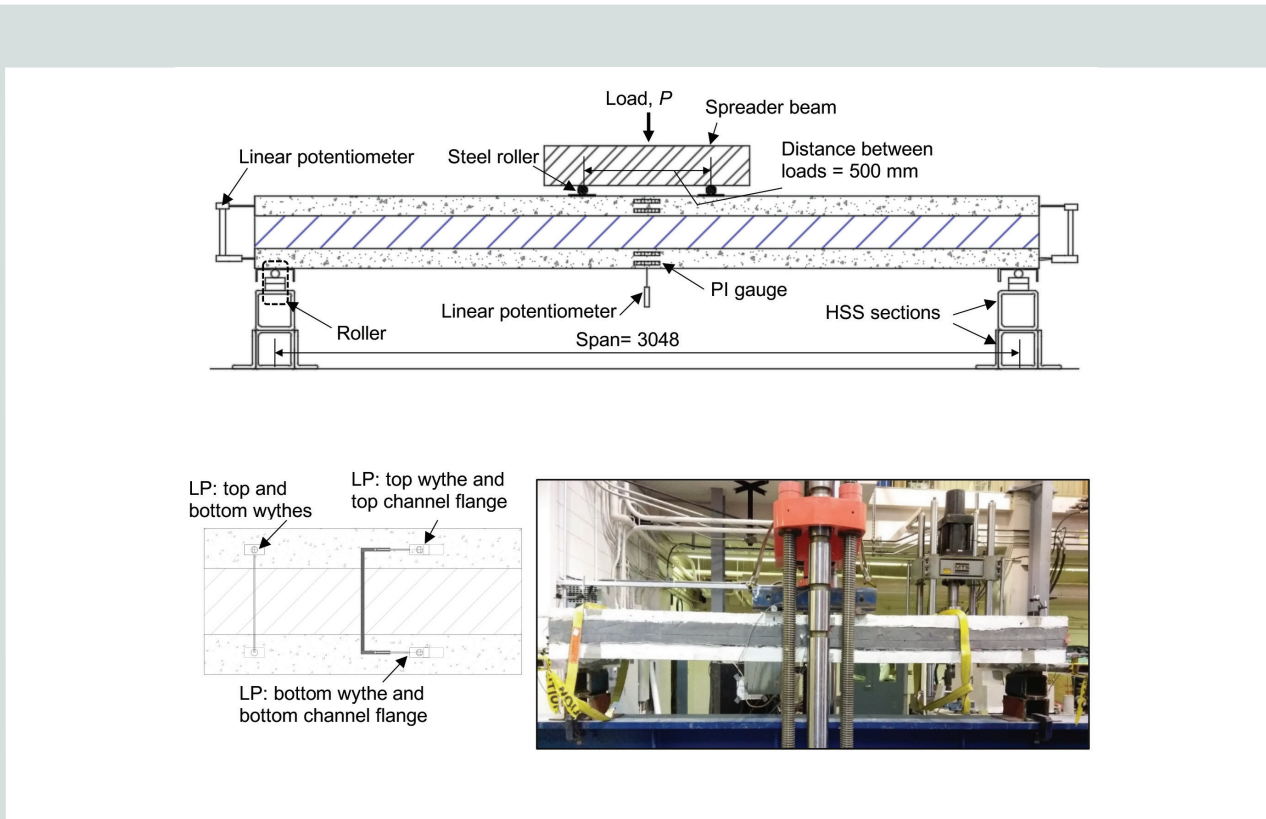


Figure 6. Test setup: schematics showing panel side (top), cross section at panel end (bottom left), and panel under testing (bottom right). Note: HSS = hollow structural section; LP = linear potentiometer. 1 mm = 0.0394 in.

both ends of the panel, the slip between the top wythe and top flange of the channel connector at both ends, and the slip between the bottom wythe and bottom flange of the channel at both ends (Fig. 6).

Four 100 mm (3.9 in.) displacement-type pi-gauge strain gauges were attached to the concrete surfaces at midspan, two on each wythe, to capture the strain gradient within the wythe (Fig. 6). Strains in the top and bottom wythe reinforcements at midspan, were measured using 5 mm (0.2 in.) long electrical resistance strain gauges attached to the longitudinal bars. For the GFRP channel section, strains were measured at the outer surface of the top flange and at the outer and inner surfaces of the bottom flange at midspan using the 5 mm long strain gauges.

Results and discussion

Table 2 provides a summary of the test results, including cracking and maximum loads, failure modes, and average slip values at failure. The following sections discuss the test results in detail.

Load-deflection responses and failure modes

Figure 7 compares the experimental load P with midspan deflection Δ for the five tested panels (solid lines). The figure also shows the theoretical prediction curves (dotted lines) based on the FEA using a software program, which are discussed in the companion paper.¹⁶ These predictions are shown for the actual partially composite case (FE) and for the hypothetical noncomposite (FE-NC) and fully composite (FE-FC) cases.

Figure 7 shows that prior to concrete cracking, panels with continuous channel connectors (specimens CR, HR, and DR)

had a stiffness comparable to that of a fully composite case. However, once cracking occurred, the panel stiffness reduces significantly to a level similar to that of a noncomposite case. Failure for these panels was governed primarily by compressive crushing of the GFRP channel connector at the top flange, which was then followed by a secondary delamination in the web and sometimes tension failure in the bottom flange. This can be seen in **Fig. 8** from experimental observations after removing the insulation layer (FEA simulations are also shown in the same figure). The failure was located near the midspan section, with FEA models showing the failure initiating at approximately 200 mm (7.9 in.) from midspan. A large drop in load, indicative of brittle failure, appeared immediately after the crushing (Fig. 7).

For panels DC and TR, the pre- and postcracking stiffnesses are generally between those of the fully composite and noncomposite cases (Fig. 7). Panel DC reached a peak load until one of the discrete channel segments at one end pulled out of the bottom wythe at a maximum load $P_{max} = 28$ kN (6.3 kip) (Fig. 8). After that, the load decreased gradually and several channel segments at the same shear span failed by web shear (Fig. 8) in a consecutive manner leading to a large deflection. Panel TR failed by tensile rupturing of the longitudinal reinforcement of the bottom concrete wythe after excessive yielding, leading to a large increase in deflection and ductility (Fig. 7).

Effects of wythe reinforcement ratio The reinforcement ratio ρ_s in the wythe was investigated in panels CR, HR, and DR by varying ρ_s from 0.17% to 0.68%. **Figure 9** shows the P - Δ response for the three panels. The precracking stiffness of the three panels is almost identical; however, after cracking, the panel stiffness increased slightly as ρ_s increased. Table 2 summarizes the cracking loads P_{cr} in each of the wythes for

Table 2. Summary of test results of flexural concrete sandwich panels

Specimen code	Cracking load P_{cr} , kN		Maximum load P_{max} , kN	Failure mode	Average slip at failure δ , mm			Total slip δ_4 , mm at 21.7 kN
	Bottom wythe	Top wythe			δ_1	δ_2	δ_3	
HR	16.3	22.6	64.3	CC, DL	11.6	6.1	19.6	3.4
CR	11.1	14.0	61.1	CC, DL	8.2	4.7	14.6	3.7
DR	15.8	20.6	85.4	CC, DL	11.6	7.9	34.2	6.5
DC	10.8	15.3	28.0	SH	n.d.	0.1	2.5	2.8
TR	9.4	15.1	21.7	RR	n.d.	n.d.	12.8	25.9

Note: CC = compressive crushing of channel connector at top flange and upper part of web; CR = specimen with continuous GFRP shear connectors and a wythe reinforcement ratio equal to 0.34%; DC = specimen with discontinuous GFRP shear connectors and a wythe reinforcement ratio equal to 0.34%; DL = delamination of FRP layers in the web of channel connector; DR = specimen with continuous GFRP shear connectors and a wythe reinforcement ratio equal to 0.68%; GFRP = glass-fiber-reinforced polymer; HR = specimen with continuous GFRP shear connectors and a wythe reinforcement ratio equal to 0.17%; n.d. = no data due to gauge malfunction; RR = rupture of longitudinal flexural reinforcement in bottom wythe; SH = shear failure in the discrete channel connector; TR = control specimen with steel shear connectors; δ_1 = average slip between top concrete wythe and top flange of channel connector; δ_2 = average slip between bottom concrete wythe and bottom flange of channel connector; δ_3 = average slip between concrete wythes; δ_4 = total slip between concrete wythes at 21.7 kN (maximum load of panel TR). 1 mm = 0.0394 in.; 1 kN = 0.225 kip.

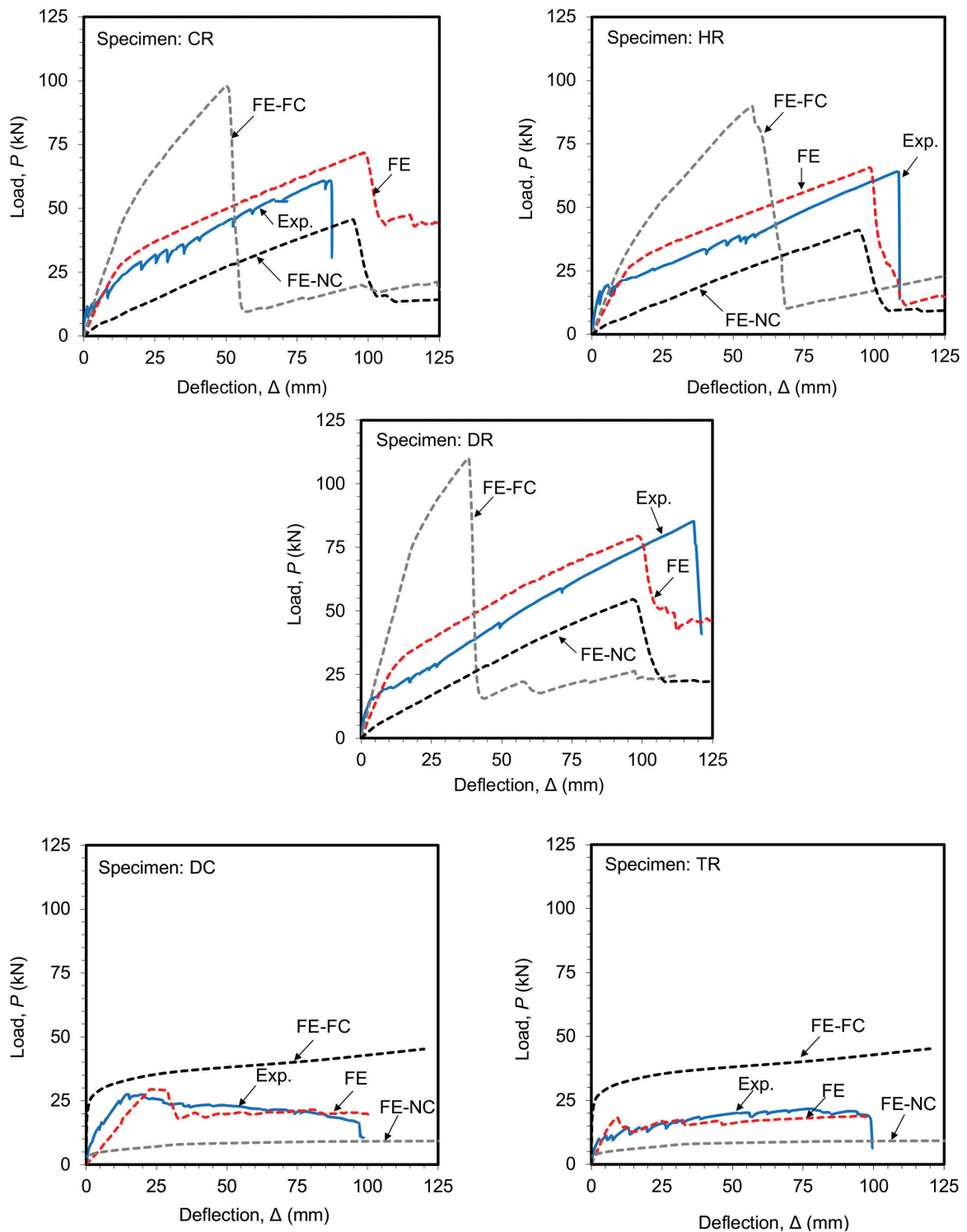


Figure 7. Comparison of load and midspan deflection among experimental, finite element prediction, noncomposite finite element, and fully composite finite element. Note: CR = specimen with continuous GFRP shear connectors and a wythe reinforcement ratio equal to 0.34%; DC = specimen with discontinuous GFRP shear connectors and a wythe reinforcement ratio equal to 0.34%; DR = specimen with continuous GFRP shear connectors and a wythe reinforcement ratio equal to 0.68%; Exp. = experimental; FE = finite element prediction; FE-FC = fully composite finite element; FE-NC = noncomposite finite element; GFRP = glass-fiber-reinforced polymer; HR = specimen with continuous GFRP shear connectors and a wythe reinforcement ratio equal to 0.17%; TR = control specimen with steel shear connectors. 1 mm = 0.0394 in.; 1 kN = 0.225 kip.

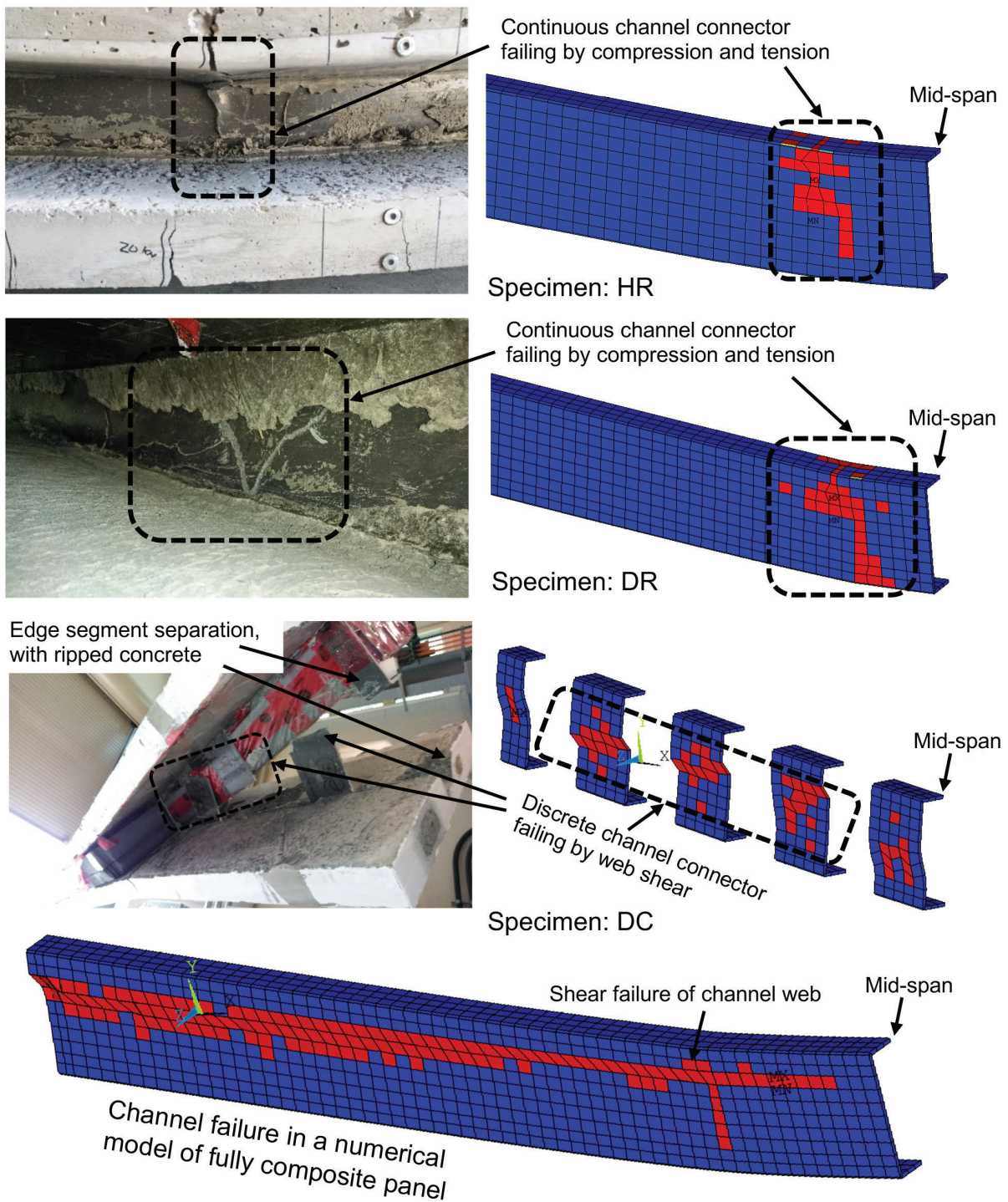


Figure 8. Channel connector failure modes, as observed in tests and predicted by finite element models (represented by the red colored elements and deformed shape). Note: DC = specimen with discontinuous GFRP shear connectors and a wythe reinforcement ratio equal to 0.34%; DR = specimen with continuous GFRP shear connectors and a wythe reinforcement ratio equal to 0.68%; GFRP = glass-fiber-reinforced polymer; HR = specimen with continuous GFRP shear connectors and a wythe reinforcement ratio equal to 0.17%.

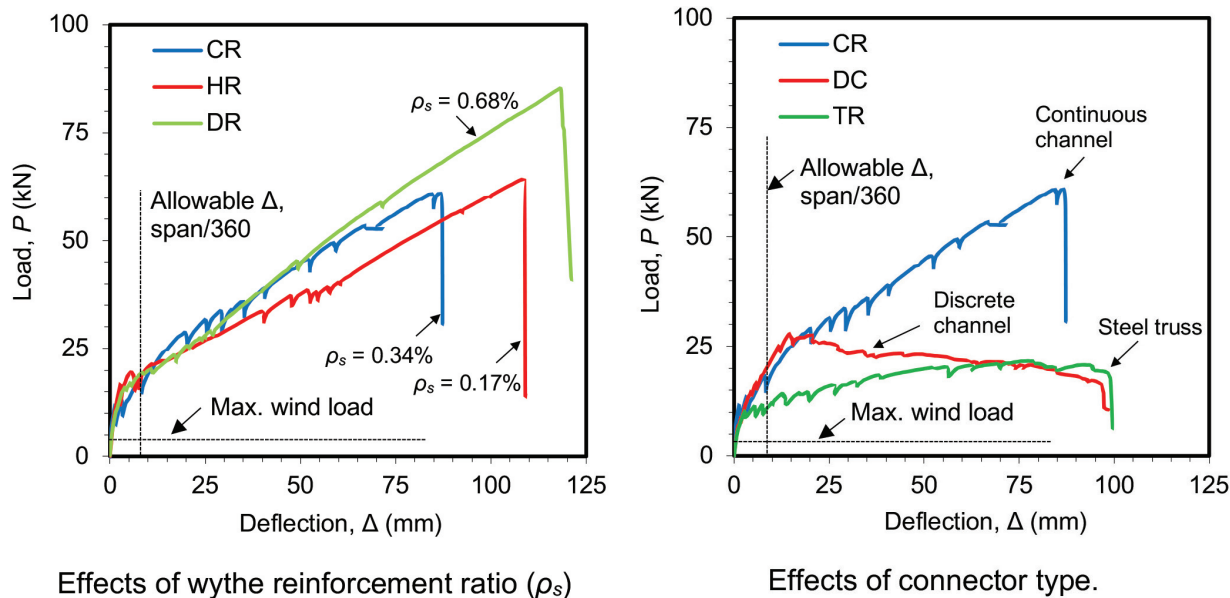


Figure 9. Comparison of experimental load and midspan deflection, showing the effects of wythe reinforcement ratio and connector type. Note: CR = specimen with continuous GFRP shear connectors and a wythe reinforcement ratio equal to 0.34%; DC = specimen with discontinuous GFRP shear connectors and a wythe reinforcement ratio equal to 0.34%; DR = specimen with continuous GFRP shear connectors and a wythe reinforcement ratio equal to 0.68%; GFRP = glass-fiber-reinforced polymer; HR = specimen with continuous GFRP shear connectors and a wythe reinforcement ratio equal to 0.17%; TR = control specimen with steel shear connectors. 1 mm = 0.0394 in.; 1 kN = 0.225 kip.

all specimens. In all specimens, the bottom wythe cracked first and at a lower load than that for the top wythe.

Although the failure mode of the three specimens is identical, the maximum load P_{max} varies with ρ_s . P_{max} increased by 33% when ρ_s increased from 0.17% to 0.68% (Table 2). However, no increase in P_{max} occurred when ρ_s increased from 0.17% to 0.34% despite the increase in stiffness. This may be because ultimate loads in this system are governed by compression failure of the GFRP section and because the system is partially composite.

The maximum service and factored wind pressures in the Canadian building code²² are 1.37 and 2.9 kPa (0.2 and 0.4 psi), respectively (peak 50-year return period). These pressures are equivalent to 1.5 and 3.1 kN (0.3 and 0.7 kip) of concentrated loads, respectively, for the four-point testing used in this study. Figure 9 shows the factored load level for comparison with experimental results. The failure loads P_{max} were all well above the maximum factored load. Also, the deflections under the service load were well below the deflection limit of span $L/360$ (Fig. 9).

Effects of connector type Figure 9 shows the P - Δ curves for the panels with three connector types: a continuous GFRP channel (specimen CR), a discontinuous GFRP channel (specimen DC), and a steel truss (specimen TR). Prior to cracking of the bottom wythe, which occurred at $P_{cr} = 11.1, 10.8,$ and

9.4 kN (2.5, 2.4, and 2.1 kip) for specimens CR, DC, and TR, respectively, the panel stiffnesses were almost identical. After cracking, the stiffness of panel TR began dropping due to propagation of cracking and yielding of wythe reinforcement. The stiffnesses of panels CR and DC were comparable until specimen DC reached its maximum load of $P_{max} = 28$ kN (6.3 kip) and its stiffness reduced gradually thereafter (Fig. 9). Hypothetically, if the web shear failure in the discrete channel segments did not occur, specimen DC would have resisted more load and continued to behave similarly to the panel with a continuous channel.

In comparisons of the maximum load P_{max} of the three panels, specimen CR resisted the highest load (Table 2). The superior performance of specimen CR is attributed primarily to the contribution of the continuous GFRP flanges of the C section inside the wythes as well as the GFRP web to the overall flexural strength. This flexural contribution does not occur in the discrete channel sections or the steel truss system. The contribution of the channel connector to flexure was estimated using Eq. (1), which is based on the ASCE LRFD prestandard for pultruded FRP structures:²³

$$M_n = \min \left\{ \left[\frac{F_{L,f} (E_{L,f} I_f + E_{L,w} I_w)}{r} \right] \right\}$$

$$\left[\frac{F_{L,w}(E_{L,f}I_f + E_{L,w}I_w)}{y_w E_{L,w}} \right] \quad (1)$$

where

- M_n = nominal moment capacity of FRP section
- $F_{L,f}$ = longitudinal strength of flange
- $E_{L,f}$ = longitudinal modulus of flange
- I_f = moment of inertia of flange about the axis of bending
- $E_{L,w}$ = longitudinal modulus of web
- I_w = moment of inertia of web about the axis of bending
- y_f = distance from the neutral axis to the extreme fiber of flange
- $F_{L,w}$ = longitudinal strength of web
- y_w = distance from the neutral axis to the extreme fiber of web

After calculating M_n using the geometrical inputs of the channel and material properties reported previously, where compression failure governs, the maximum load of the channel P_{max} was then determined from the four-point bending configuration and was found to be 35.9 kN (8.1 kip), which is 60% of the capacity of specimen CR.

Degree of composite action

The degree of composite action k , which is a measure of how much shear the connector is able to transfer between wythes,

was determined for the tested panels using the load method defined by Eq. (2):

$$k = \frac{P_{max}(\text{test}) - P_{max}(\text{NC})}{P_{max}(\text{FC}) - P_{max}(\text{NC})} \times 100 \quad (2)$$

where

- $P_{max}(\text{test})$ = maximum load from test
- $P_{max}(\text{NC})$ = maximum load from the numerical model for the noncomposite case
- $P_{max}(\text{FC})$ = maximum load from the numerical model for the fully composite case

Table 3 lists the values of k for each of the tested panels. Generally, panels with channel connectors exhibited the highest composite degrees. For panels HR, CR, and DR featuring a continuous channel connector, k was on average 51%. The wythe reinforcement ratio in these panels seems to have negligible effects on the degree of composite action, but P_{max} for the noncomposite and fully composite theoretical cases seems to increase with increasing ρ_s (Table. 3). For the discontinuous channel connector specimen (DC), k was also 51%. The panel with a steel truss connector (specimen TR) had the lowest composite degree, $k = 33\%$; this represents 65% of the k value of panels with GFRP channel connectors. In addition, the maximum loads of the panel with a truss connector were also significantly lower than that of the panel with a continuous channel connector (specimen CR), with 22% for the noncomposite and 46% for the fully composite cases (Table 3).

Load-relative slip responses

Figure 10 compares the load P and slip δ between the top and bottom concrete wythes on either end of the panels. The figure shows that slip was negligible when P was smaller than the cracking loads of the bottom wythe (reported in Table 2). Once

Table 3. Finite element correlation with experimental results and degree of composite action

Specimen code	Maximum load P_{max} , kN		Load difference between test and model, %	$P_{max}(\text{NC})$, kN	$P_{max}(\text{FC})$, kN	Degree of composite action k , %
	Test	Finite element model				
HR	64.3	65.6	2.0	40.8	89.7	48
CR	61.1	71.8	17.3	45.4	98.0	30 (50)*
DR	85.3	79.4	6.9	54.5	109.9	56
DC	28.0	29.4	5.0	10.0	45.2	51
TR	17.9	19.7	10.5	10.0	45.2	33

Note: CR = specimen with continuous GFRP shear connectors and a wythe reinforcement ratio equal to 0.34%; DC = specimen with discontinuous GFRP shear connectors and a wythe reinforcement ratio equal to 0.34%; DR = specimen with continuous GFRP shear connectors and a wythe reinforcement ratio equal to 0.68%; FC = fully composite; GFRP = glass-fiber-reinforced polymer; HR = specimen with continuous GFRP shear connectors and a wythe reinforcement ratio equal to 0.17%; NC = noncomposite; TR = control specimen with steel shear connectors. 1 kN = 0.225 kip.

*Calculated using $P_{max}(\text{FE})$ in place of $P_{max}(\text{test})$.

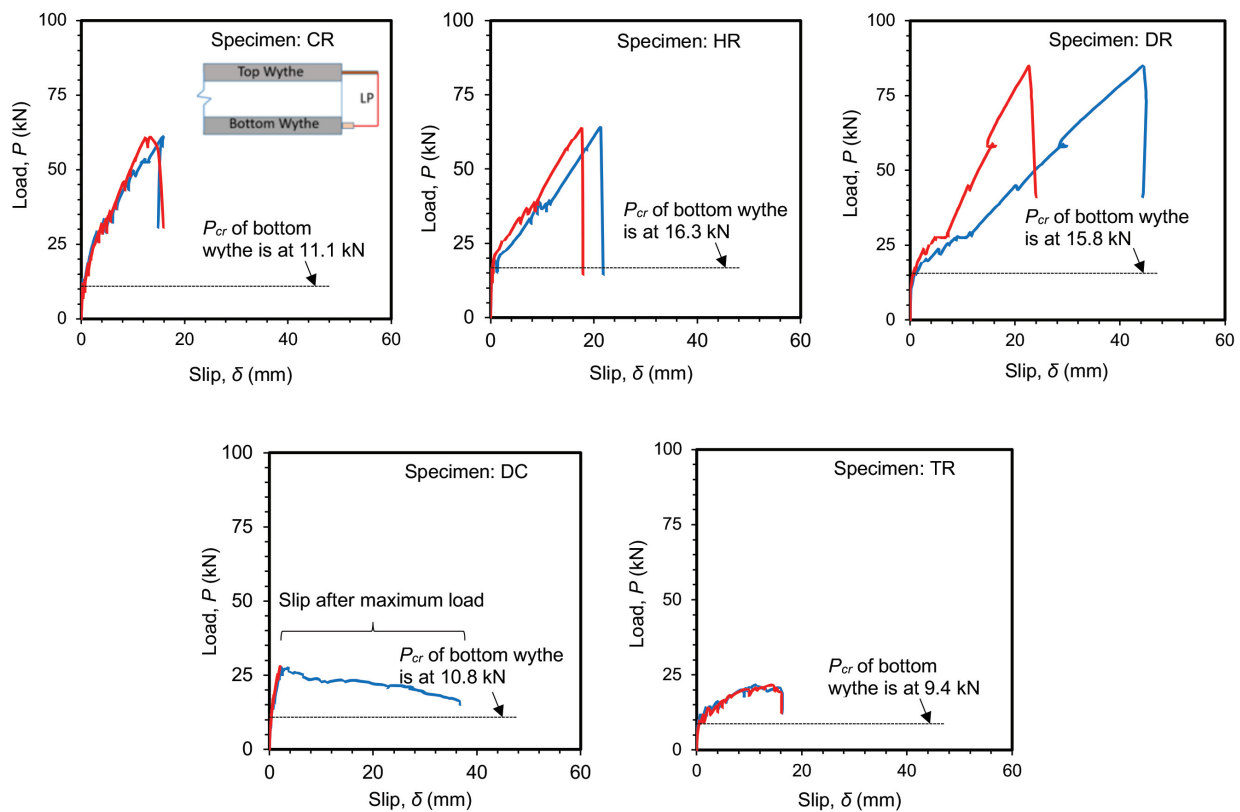


Figure 10. Load versus wythe-to-wythe slipping for all tested panels. Note: CR = specimen with continuous GFRP shear connectors and a wythe reinforcement ratio equal to 0.34%; DC = specimen with discontinuous GFRP shear connectors and a wythe reinforcement ratio equal to 0.34%; DR = specimen with continuous GFRP shear connectors and a wythe reinforcement ratio equal to 0.68%; GFRP = glass-fiber-reinforced polymer; HR = specimen with continuous GFRP shear connectors and a wythe reinforcement ratio equal to 0.17%; LP = linear potentiometer; P_{cr} = cracking load; TR = control specimen with steel shear connectors. 1 mm = 0.0394 in.; 1 kN = 0.225 kip.

cracking occurred, more slip developed between the wythes. Table 2 lists the wythe-to-wythe slip at maximum load P_{max} . Comparing the panels with varying wythe reinforcement ratios, panel DR (with $\rho_s = 0.68\%$) had the greatest average slip at $\delta = 34.2$ mm (1.35 in.) compared with an average slip of $\delta = 17$ mm (0.67 in.) for the other two specimens. The maximum average slip in panel TR, which had a steel truss connector, was 12.8 mm (0.50 in.), slightly less than the average slip of 14.6 mm (0.57 in.) in panel CR, which had a continuous GFRP channel, at their respective P_{max} values. Panel DC, which had a discontinuous GFRP channel, experienced the smallest slip, 2.5 mm (0.1 in.) at P_{max} . This small slip was attributed to the lateral restraint provided by concrete, which surrounded the embedded channel segments on all sides. After reaching maximum load, slip continued to develop at the side that did not experience shear failure in the channel segments (Fig. 10).

Figure 11 compares the load and slip between the top wythe and top channel flange and between the bottom wythe and bottom channel flange for the three panels with continuous GFRP channels at both ends of the panel. In these panels,

the bottom GFRP flange always slipped out of the bottom wythe (indicated by the positive sign in Fig. 11 and shown in **Fig. 12**) while the top GFRP flange slipped in (indicated by the negative sign in Fig. 11 and shown in Fig. 12). Figure 12 also shows the predicted slip from the nonlinear FEA models, which will be discussed in the companion paper.¹⁶ Generally, slippage of the top flange was greater than that of the bottom one for all three panels.

Effect of connector type To assess connector effectiveness in shear transfer, slip should be compared at the same load level. The total slip (that is, both ends added) of specimens CR, DC, and TR with continuous channels, discrete channels, and a steel truss, respectively, was compared at the smallest maximum load of the three, which was 21.7 kN (4.9 kip) for specimen TR. These values were 3.7, 2.7, and 25.9 mm (0.15, 0.11, and 1.02 in.) for CR, DC, and TR, respectively (Table 2). The channel connector was more effective than the steel truss, as evidenced by the significantly smaller slip. Also, the discrete channel sections provided slightly less slip, being surrounded on four sides by concrete, unlike the continuous channel. In this

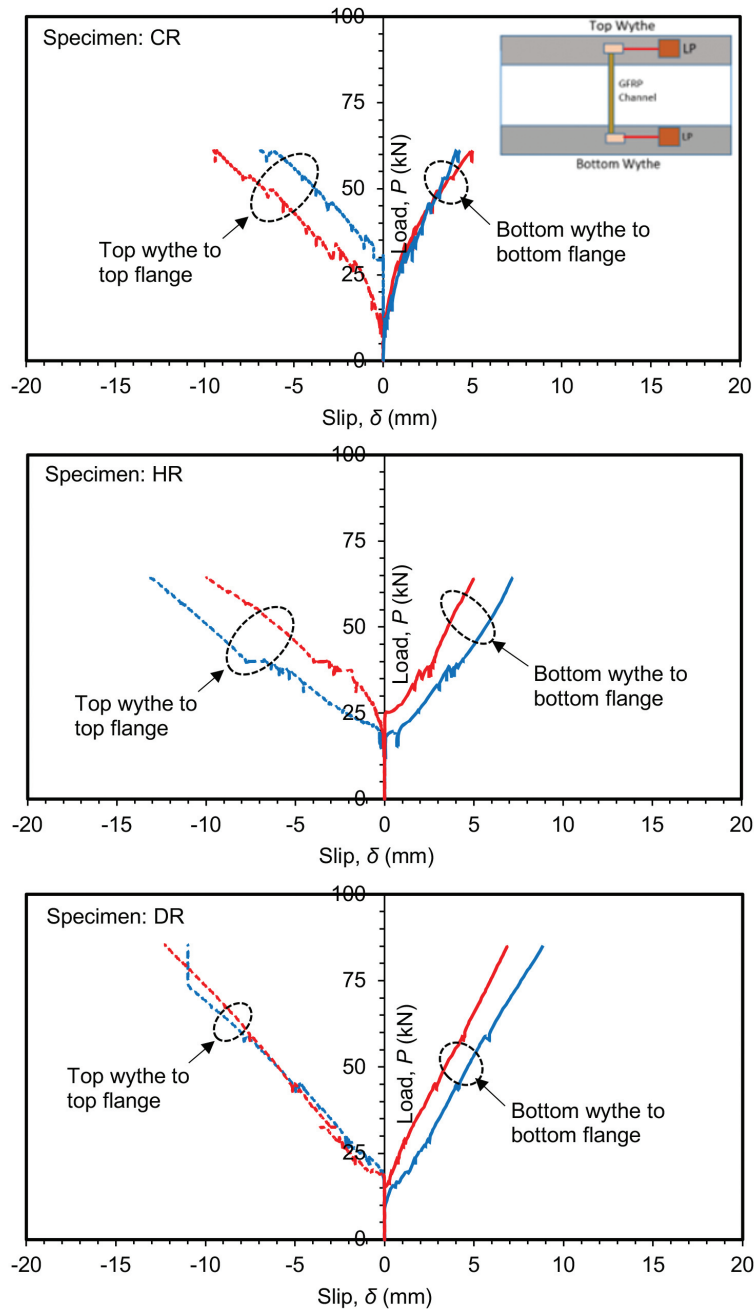


Figure 11. Load versus slip for the panels with continuous channel connector measured from top wythe to top channel flange and from bottom wythe to bottom channel flange. Note: CR = specimen with continuous GFRP shear connectors and a wythe reinforcement ratio equal to 0.34%; DR = specimen with continuous GFRP shear connectors and a wythe reinforcement ratio equal to 0.68%; GFRP = glass-fiber-reinforced polymer; HR = specimen with continuous GFRP shear connectors and a wythe reinforcement ratio equal to 0.17%; LP = linear potentiometer. 1 mm = 0.0394 in.; 1 kN = 0.225 kip.

case, the 2.7 mm was due to shear deformation of the channel and did not include slip between the channel and concrete.

Load-strain responses

Figure 13 shows midspan strains at the top and bottom flanges of the channel connector as well as in the top and

bottom wythe reinforcements for the panels with continuous channel connectors. The channel strains were consistently in compression at the top flange and in tension at the bottom flange, while wythe reinforcement strains depended on the location of the neutral axis for the wythe containing the instrumented reinforcement. The maximum tensile and compressive strains in the channel, 0.013 (at strain gauge

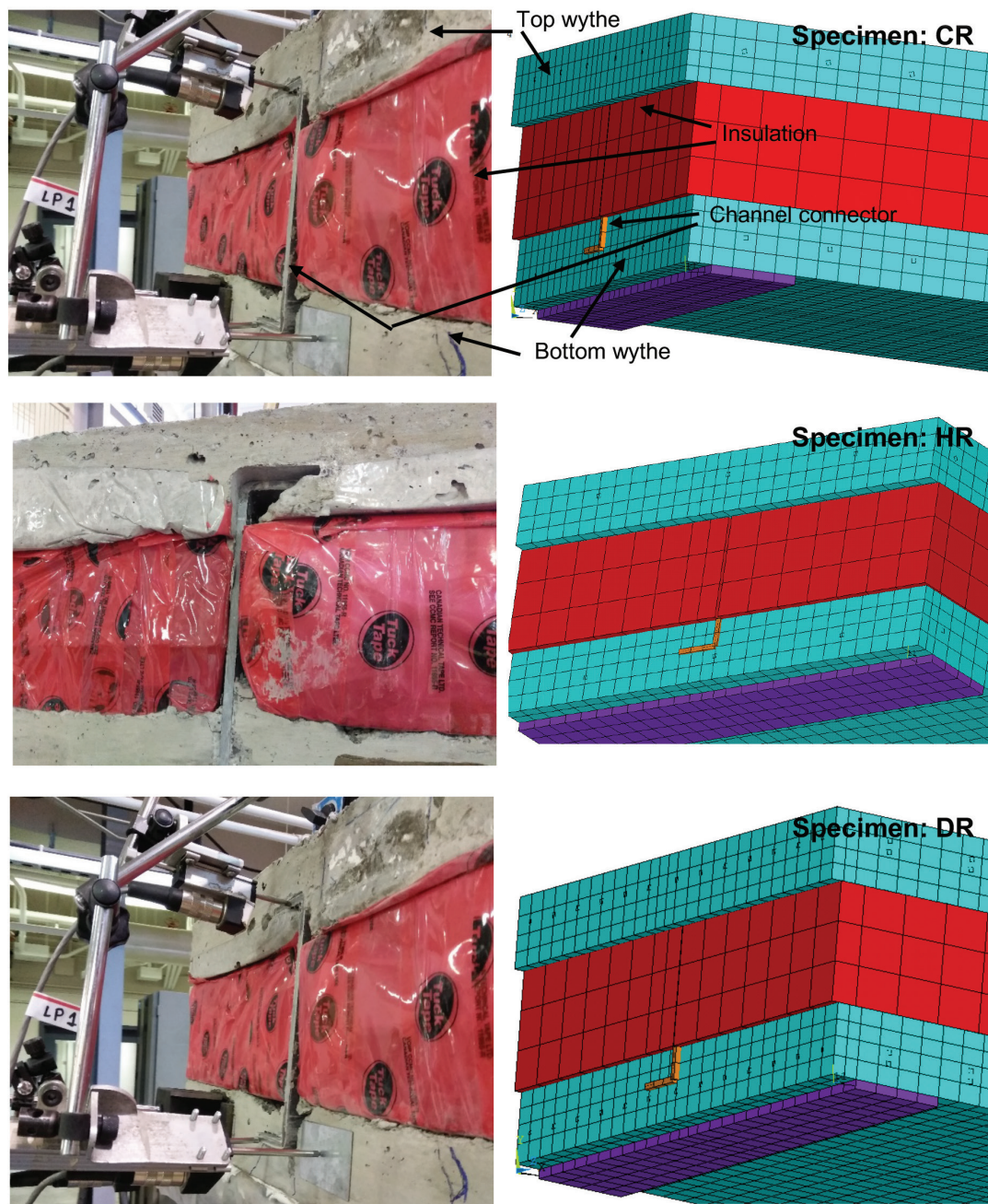


Figure 12. Panel end slipping, as observed from tests or predicted by finite element models, for the panels with continuous channel connector. Note: CR = specimen with continuous GFRP shear connectors and a wythe reinforcement ratio equal to 0.34%; DR = specimen with continuous GFRP shear connectors and a wythe reinforcement ratio equal to 0.68%; GFRP = glass-fiber-reinforced polymer; HR = specimen with continuous GFRP shear connectors and a wythe reinforcement ratio equal to 0.17%.

3, SG3) and 0.08 (at strain gauge 1, SG1), respectively, were slightly less than the rupture strains of 0.017 (tension) and 0.011 (compression), measured in the coupon tests. Although channel failure is imminent at the midspan section, as can be seen from the previously mentioned strains, the channel actually failed in compression near the loading point.

Because the pi gauges mounted on the wythe surface to measure concrete strains and variation of the neutral axis were not functioning properly, the FEA model was used to determine the strain profiles at midspan instead. **Figure 14** shows the strain profiles at midspan at three loads— $P = 15, 30,$ and 60 kN (3.4, 6.7, and 13.5 kip)—comparing all tested panels. Specimens DC and TR failed before reaching

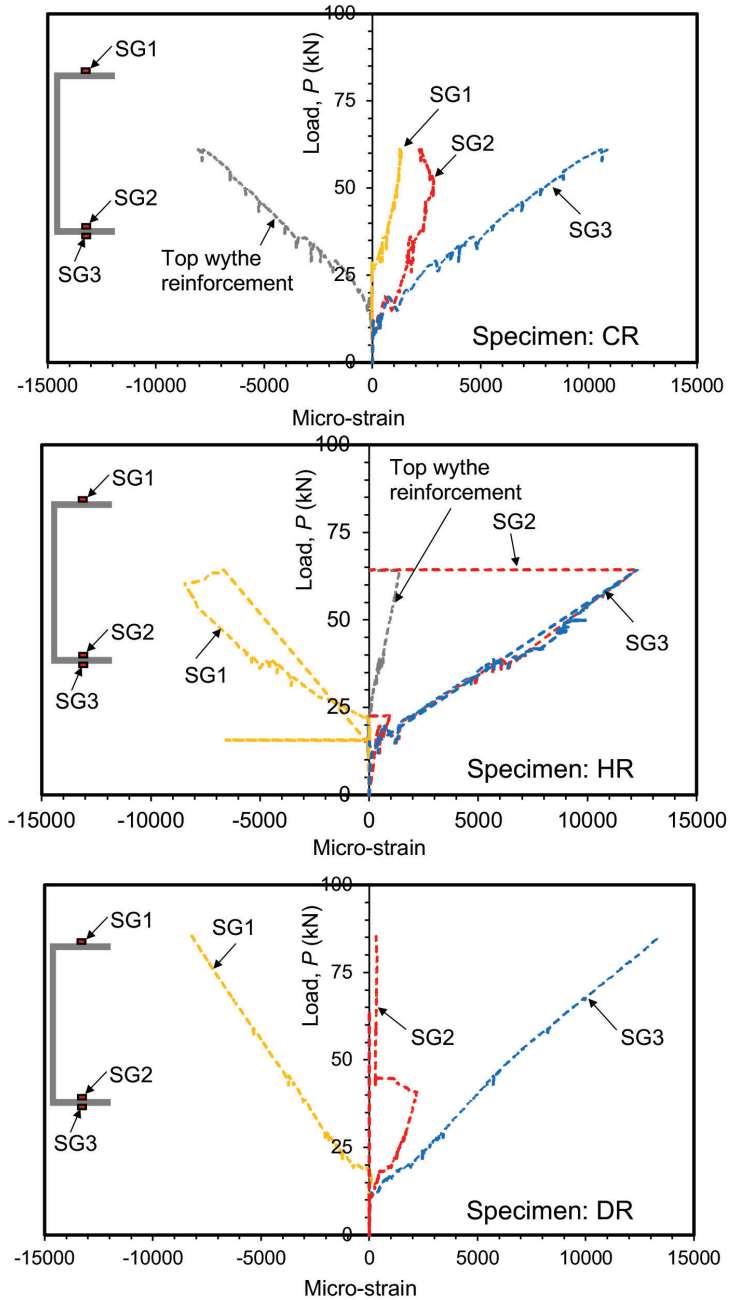


Figure 13. Load versus midspan strain in channel connector and wythe reinforcement for the panels with continuous channel connector. Note: CR = specimen with continuous GFRP shear connectors and a wythe reinforcement ratio equal to 0.34%; DR = specimen with continuous GFRP shear connectors and a wythe reinforcement ratio equal to 0.68%; GFRP = glass-fiber-reinforced polymer; HR = specimen with continuous GFRP shear connectors and a wythe reinforcement ratio equal to 0.17%; SG = strain gauge. 1 kN = 0.225 kip.

$P = 30$ kN and therefore were not included in the last two comparisons. All specimens showed a partial composite behavior, where three neutral axes exist for the top wythe, the channel, and the bottom wythe (Fig. 14). The location of the neutral axis for the top wythe was approximately 20 mm (0.8 in.) from its top fiber. For the channel it was located near its midheight. For the bottom wythe, the neutral axis

was located either at its top fiber or slightly above within the channel. In a comparison of specimens with different connectors at $P = 15$ kN, the specimen with the discrete channel (DC) had higher strains than specimens CR and TR. In a comparison of specimens with various wythe reinforcement ratios, strain decreased in general with increasing ρ_s , as expected (Fig. 14).

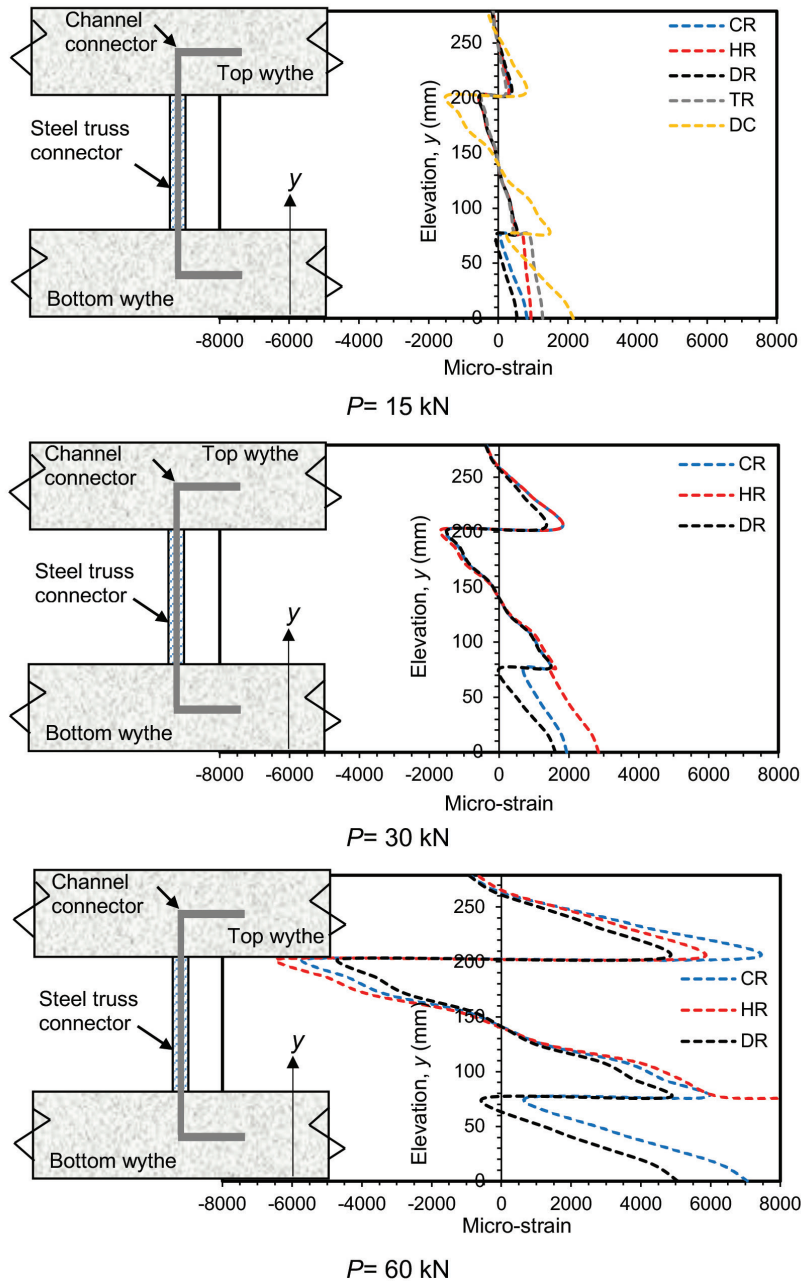


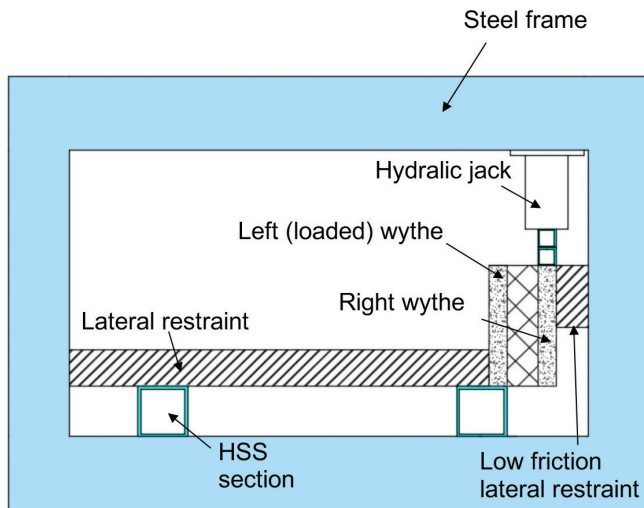
Figure 14. Midspan strain profile at different loads for all tested panels. Note CR = specimen with continuous GFRP shear connectors and a wythe reinforcement ratio equal to 0.34%; DC = specimen with discontinuous GFRP shear connectors and a wythe reinforcement ratio equal to 0.34%; DR = specimen with continuous GFRP shear connectors and a wythe reinforcement ratio equal to 0.68%; GFRP = glass-fiber-reinforced polymer; HR = specimen with continuous GFRP shear connectors and a wythe reinforcement ratio equal to 0.17%; TR = control specimen with steel shear connectors. 1 mm = 0.0394 in.; 1 kN = 0.225 kip.

Push-off shear and bond tests

Two 500 mm (19.7 in.) long panel segments, S1 and S2, were saw cut from an additional panel identical to specimen CR in the bending tests and were tested under single shear loading. Different boundary conditions were used to determine both the shear strength of the GFRP channel connector

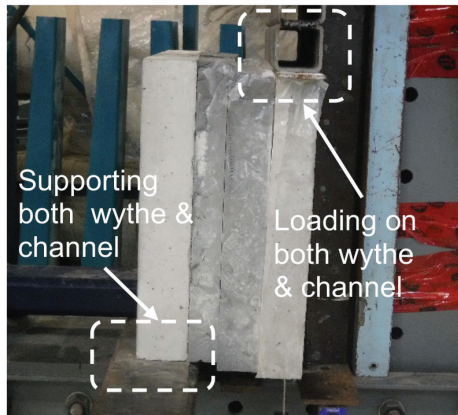
and the bond strength of the concrete–channel interface.

Figure 15 shows the schematics and a picture of the test setup, which consisted of a self-reacting steel frame, lateral restraints, loading on top of one wythe using a 300 kN (67.4 kip) capacity hydraulic jack, and supporting the other wythe at the bottom. The specimens were tested in a vertical position. The lateral restraints, which consisted of hollow

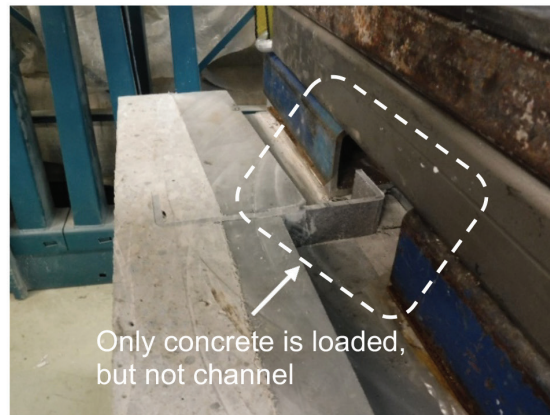


Schematics of test setup

Picture of test setup



Specimen S1 for testing shear strength of GFRP channel connector



Specimen S2 for testing bond strength of concrete-channel interface

Figure 15. Push-off tests. Note: GFRP = glass-fiber-reinforced polymer; HSS = hollow structural section; S1 = specimen for testing shear strength of GFRP channel connector; S2 = specimen for testing bond strength of concrete-GFRP channel interface.

structural sections (HSSs), ensured that the specimen could only move vertically (Fig. 15). Friction between the loaded wythe and lateral restraint was minimized by applying a lubricant at the interface.

Support and loading schemes differed in each of the two specimens. In specimen S1 (Fig. 15), bearing of the vertical support and loading was applied to both the concrete and the GFRP channel connector to establish the longitudinal shear behavior and shear strength of the GFRP connector. In specimen S2, support was similar to that in specimen S1 (that is, bearing on both wythe and channel) but the vertical load was applied to the concrete wythe only and not to the channel (Fig. 15) to establish bond strength.

Figure 16 compares the load P with the relative longitudinal deflection between the concrete wythes for the two tested specimens. Failure of specimen S1 was due to excessive shear deformation in the web of the channel, and failure for specimen S2 was due to excessive slippage between the concrete and the channel (Fig. 15).

The channel shear strength was estimated in S1 by dividing the maximum load P_{max} of the specimen by the longitudinal cross-sectional area of the web and was found to be 39 MPa (5.7 ksi). The bond strength τ_{max} of the GFRP channel connector to the concrete was estimated by dividing P_{max} of specimen S2 by the channel interfacial area in contact with the concrete and was found to be 0.28 MPa (0.04 ksi).

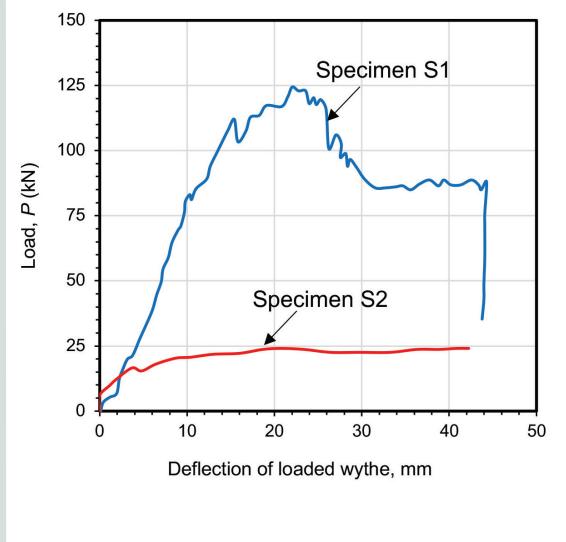


Figure 16. Load versus deflection of left (loaded) wythe curve in push-off specimens. Note: S1 = specimen for testing shear strength of GFRP channel connector; S2 = specimen for testing bond strength of concrete-GFRP channel interface. 1 mm = 0.0394 in.; 1 kN = 0.225 kip.

Conclusion

In this study, a new C-shaped GFRP pultruded channel shear connector for precast concrete sandwich panels was investigated. The connector was intended to increase the structural efficiency of the precast concrete sandwich panel while maintaining high thermal efficiency due to the connector's low thermal conductivity. Five half-scale precast concrete sandwich panels were tested in four-point bending and reported in this paper, which is part 1 of two papers, with the companion paper¹⁶ focused on numerical modeling and a parametric study. Three panels with continuous GFRP channel connectors included different reinforcement ratios ρ_s in the concrete wythes. In the fourth panel, multiple segments of the GFRP channel, spaced apart, were used to further reduce thermal bridging. The fifth panel, which was used for comparison, had a conventional steel truss connector with a diagonal stiffness equal to that of the continuous channel. The responses of all panels were compared and assessed in reference to the theoretical fully composite and noncomposite responses. In addition, two panel segments measuring 500 mm (19.7 in.) in length were tested under single shear with different boundary conditions to determine the longitudinal shear strength of the channel connector and the bond strength of the concrete-channel interface. The following conclusions are drawn from this experimental study:

- The continuous GFRP channel at all reinforcement ratios tested outperformed other connectors. It resulted in a

panel maximum load P_{max} 2.56 and 4.0 times that for the discontinuous channel and the conventional steel truss, respectively. The panel with discontinuous channel had similar stiffness to the one with continuous channel before failure; however, stiffness of the panel with a steel truss connector was much lower.

- All panels with continuous GFRP channels failed by crushing of the GFRP flange of the channel in the compression wythe. For the specimen with a discontinuous channel connector, the GFRP channel segments failed by web shear after the edge segment pulled out the bottom concrete wythe in one shear span. In the specimen with a steel truss connector, failure occurred by tension rupture of the steel reinforcement in the bottom wythe.
- For the three panels with continuous channels and different reinforcement ratio in the wythe, maximum load P_{max} increased by 33%, when ρ_s increased from 0.17% to 0.68%. No gain was observed between ρ_s of 0.17% and 0.34%, which may be attributed to the GFRP compression failure mode and the partial composite action of the system.
- The degree of composite action for each panel was calculated and found to be about 50% for both continuous and discontinuous GFRP channels, whereas that of the steel truss was only 33%.
- The continuous GFRP channel not only increased the degree of composite action of the wall compared with the steel truss connector but also contributed significantly to flexural strength by means of the embedded GFRP flanges. This contribution was calculated to be 49% of the overall panel strength.
- The total end slip between concrete wythes is a good measure for comparing efficiency of different connectors. This slip at the peak load of the panel with a steel connector was 25.9 mm (1.02 in.), while for panels with continuous and discrete channels it was 3.7 and 2.8 mm (0.15 and 0.11 in.), respectively, at the same load. This clearly showed that the GFRP channel connector was more effective than the steel truss. The discrete channel provided slightly less slip being surrounded by concrete from four sides.
- The concrete bond strength of the GFRP channel, determined from the single shear push-off test, was 0.28 MPa (0.04 ksi) while the longitudinal shear strength of the GFRP channel was 39 MPa (5.7 ksi).

Acknowledgments

The authors wish to acknowledge the financial support provided by the Canadian Precast/Prestressed Concrete Institute (CPCI) for this project and the advocacy of CPCI president Robert Burak for research and innovation.

References

1. Einea, A., D. C. Salmon, M. K. Tadros, and T. Culp. 1994. "A New Structurally and Thermally Efficient Precast Sandwich Panel System." *PCI Journal* 39 (4): 90–101.
2. Hassan, T. K., and S. H. Rizkalla. 2010. "Analysis and Design Guidelines of Precast, Prestressed Concrete, Composite Load-Bearing Sandwich Wall Panels Reinforced with CFRP Grid." *PCI Journal* 55 (2): 147–162.
3. Tomlinson, D. G., N. Teixeira, and A. Fam. 2016. "New Shear Connector Design for Insulated Concrete Sandwich Panels Using Basalt Fiber Reinforced Polymer Bars." *Journal of Composites for Construction* 20 (4). doi: 10.1061/(ASCE)CC.1943-5614.0000662.
4. PCI Committee on Precast Concrete Sandwich Wall Panels. 2011. "State of the Art of Precast/Prestressed Concrete Sandwich Wall Panels." *PCI Journal* 56 (2): 131–176.
5. Tomlinson, D., and A. Fam. 2015. "Flexural Behavior of Precast Concrete Sandwich Wall Panels with Basalt FRP and Steel Reinforcement." *PCI Journal* 60 (6): 51–71.
6. Maximos, H. N., W. A. Pong, and M. K. Tadros. 2007. "Behavior and Design of Composite Precast Prestressed Concrete Sandwich Panels with NU-Tie." University of Nebraska–Lincoln, final report.
7. Bush, T. D., and G. L. Stine. 1994. "Flexural Behavior of Composite Precast Concrete Sandwich Panels with Continuous Truss Connectors." *PCI Journal* 39 (2): 112–121.
8. Salmon, D. C., A. Einea, M. K. Tadros, and T. D. Culp. 1997. "Full Scale Testing of Precast Concrete Sandwich Panels." *ACI Structural Journal* 94 (4): 354–362.
9. Frankl, B. A., G. W. Lucier, T. K. Hassan, and S. H. Rizkalla. 2011. "Behavior of Precast, Prestressed Concrete Sandwich Wall Panels Reinforced with CFRP Shear Grid." *PCI Journal* 56 (2): 42–54.
10. Frankl, B. A. 2008. "Structural Behavior of Insulated Precast Prestressed Concrete Sandwich Panels Reinforced with CFRP Grid." MSc thesis, Department of Civil, Construction and Environmental Engineering, North Carolina State University, Raleigh, NC.
11. Jawdhari, A., A. Peiris, and I. Harik. 2016. "Bond Study on CFRP Rod Panels Externally Adhered to Concrete." *Journal of Composites for Construction* 21 (4). doi: 10.1061/(ASCE)CC.1943-5614.0000765.
12. Jawdhari, A., and I. Harik. 2018. "Finite Element Analysis of RC Beams Strengthened in Flexure with CFRP Rod Panels." *Construction and Building Materials* 163: 751–766. doi: 10.1016/j.conbuildmat.2017.12.139.
13. Woltman, G., D. Tomlinson, and A. Fam. 2013. "Investigation of Various GFRP Shear Connectors for Insulated Precast Concrete Sandwich Wall Panels." *Journal of Composites for Construction* 17 (5): 711–721. doi: 10.1061/(ASCE)CC.1943-5614.0000373.
14. Tomlinson, D., and A. Fam. 2014. "Experimental Investigation of Precast Concrete Insulated Sandwich Panels with Glass Fiber-Reinforced Polymer Shear Connectors." *ACI Structural Journal* 111 (3): 595–605.
15. Tomlinson, D., and A. Fam. 2016. "Combined Loading Behavior of Basalt FRP-Reinforced Precast Concrete Insulated Partially-Composite Walls." *Journal of Composites for Construction* 20 (3). doi: 10.1061/(ASCE)CC.1943-5614.0000611.
16. Jawdhari, Akram, and Amir Fam. Forthcomign. "A New Studed Precast Concrete Sandwich Wall with Embedded Glass-Fiber-Reinforced Polymer Channel Sections: Part 2, Finite Element and Parametric Studies." *PCI Journal*.
17. ACI (American Concrete Institute) Committee 318. 2014. *Building Code Requirements for Structural Concrete (ACI 318-14) and Commentary (ACI 318R-14)*. Farmington Hills, MI: ACI.
18. ASTM Subcommittee C09.61. 2019. *Standard Practice for Making and Curing Concrete Test Specimens in the Field*. ASTM C31/C31M-19. West Conshohocken, PA: ASTM International.
19. ASTM Subcommittee C09.61. 2018. *Standard Test Method for Compressive Strength of Cylindrical Concrete Specimens*. ASTM C39/C39M-18. West Conshohocken, PA: ASTM International.
20. ASTM Subcommittee D30.04. 2017. *Standard Test Method for Tensile Properties of Polymer Matrix Composite Materials*. ASTM D3039/D3039M-17. West Conshohocken, PA: ASTM International.
21. ASTM Subcommittee A01.05. 2018. *Standard Specification for Carbon-Steel Wire and Welded Wire Reinforcement, Plain and Deformed, for Concrete*. ASTM A1064/A1064M-18a. West Conshohocken, PA: ASTM International.
22. NRCC (National Research Council of Canada). 2015. *National Building Code of Canada*. Ottawa, ON, Canada: NRCC 2015.
23. ASCE (American Society of Civil Engineers). 2010. *Pre-Standard for Load and Resistance Factor Design (LRFD) of Pultruded Fiber Reinforced Polymer (FRP) Structures*. Reston, VA: ASCE.

Notation

A_{FRP}	= cross section of the tributary area of the glass-fiber-reinforced polymer channel at an angle of 45 degrees	Δ	= deflection
A_s	= area of steel reinforcement	ρ_s	= wythe reinforcement ratio
b	= width of concrete wythe	τ_{max}	= bond strength of glass-fiber-reinforced polymer channel connector to concrete
E_{FRP}	= elastic modulus of glass-fiber-reinforced polymer channel		
$E_{L,f}$	= longitudinal modulus of flange		
$E_{L,w}$	= longitudinal modulus of web		
E_s	= elastic modulus of steel reinforcement		
f'_c	= concrete strength		
$F_{L,f}$	= longitudinal strength of flange		
$F_{L,w}$	= longitudinal strength of web		
I_f	= moment of inertia of flange about the axis of bending		
I_w	= moment of inertia of web about the axis of bending		
k	= degree of composite action		
L	= span		
M_n	= nominal moment capacity of fiber-reinforced polymer section		
P	= experimental load		
P_{cr}	= cracking load		
P_{max}	= maximum load		
$P_{max}(FC)$	= maximum load from the numerical model for the fully composite case		
$P_{max}(NC)$	= maximum load from the numerical model for the noncomposite case		
$P_{max}(test)$	= maximum load from test		
t	= wythe thickness		
y_f	= distance from the neutral axis to the extreme fiber of flange		
y_w	= distance from the neutral axis to the extreme fiber of web		
δ	= slip		

About the authors



Debrup Dutta is a former master's degree student in the Department of Civil Engineering at Queen's University in Kingston, ON, Canada.



Akram Jawdhari, PhD, is a postdoctoral fellow in the Department of Civil Engineering at Queen's University.



Amir Fam, PhD, PEng, is a professor, associate dean (research), and Graduate Studies and Donald and Sarah Munro Chair in the Faculty of Engineering and Applied Science at Queen's University.

Abstract

This paper examines the structural effectiveness of a new concrete sandwich panel with a shear connector made of glass-fiber-reinforced polymer (GFRP) pultruded channel sections intended to enhance composite action and flexural rigidity while minimizing thermal bridging. The flanges of the channel section were embedded in both wythes. Five half-scale panels ($610 \times 280 \times 3050$ mm [$24.02 \times 11.02 \times 120.08$ in.]) were tested in four-point bending, varying the connector configuration and type as well as the wythe reinforcement ratio. The connectors investigated were a continuous GFRP channel, a discrete GFRP channel consisting of multiple segments spaced apart, and a control conventional steel truss. Ancillary push-off single shear tests were conducted on 500 mm (19.7 in.) long wall segments to examine the GFRP connector shear strength and its bond strength to concrete. The panels with continuous and discrete GFRP channels achieved 4 and 2.6 times the ultimate strength of that with a steel truss, respectively. The continuous GFRP channel contributed 49% of the total flexural capacity of the wall. As the wythe reinforcement ratio increased from 0.17% to 0.68%, the ultimate load of the panels with continuous GFRP channels increased by 33%. Failure modes were compressive flange crushing for the panels with continuous GFRP channels, web shear for the panel with a discrete channel, and rupture of wythe reinforcement for the panel with steel truss. The continuous and discrete GFRP connectors provided an average degree of composite action of 50%, compared with 33% for the steel truss panel. The GFRP-concrete bond strength was 0.28 MPa (0.04 ksi).

Keywords

Composite action, concrete sandwich panel, finite element, glass-fiber-reinforced polymer, insulation, shear connector, thermal efficiency.

Review policy

This paper was reviewed in accordance with the Precast/Prestressed Concrete Institute's peer-review process.

Reader comments

Please address any reader comments to *PCI Journal* editor-in-chief Tom Klemens at tklemens@pci.org or Precast/Prestressed Concrete Institute, c/o *PCI Journal*, 8770 W. Bryn Mawr Ave., Suite 1150, Chicago, IL 60631. [P](#)